Determination of Intramolecular Chain Transfer and Midchain Radical Propagation Rate Coefficients for Butyl Acrylate by Pulsed Laser Polymerization

Anatoly N. Nikitin,[†] Robin A. Hutchinson,[‡] Michael Buback,*[,§] and Pascal Hesse[§]

Institute on Laser and Information Technologies, Svyatoozerskaya 1, Shatura, Moscow Region, 140700, Russia, Department of Chemical Engineering, Dupuis Hall, Queen's University, Kingston, Ontario K7L 3N6, Canada, and Institute for Physical Chemistry, University of Göttingen, Tammannstrasse 6, D-37077 Göttingen, Germany

Received June 26, 2007; Revised Manuscript Received September 5, 2007

ABSTRACT: A novel method to extract individual free-radical polymerization rate coefficients for butyl acrylate intramolecular chain transfer (backbiting), k_{bb}, and for monomer addition to the resulting midchain radical, k_p^t, is presented. The approach for measuring k_{bb} does not require knowledge of any other rate coefficient. Only the dispersion parameter of SEC broadening has to be determined by fitting measured MWDs or should be available from separate experiments. The method is based upon analysis of the shift in the position of the inflection point of polymer molecular weight distributions produced by a series of pulsed-laser polymerization (PLP) experiments with varying laser pulse repetition rate. The coefficient k_{bb} is determined from the onset of the sharp decrease of the apparent propagation rate coefficient (k_p^{app}) with decreasing repetition rate, an approach verified by simulation. With experiments performed between −10 and +30 °C, the estimated values are fitted well by an Arrhenius relation with pre-exponential factor $A(k_{bb}) = (4.84 \pm 0.29) \times 10^7$ s^{-1} and activation energy $E_a(k_{bb}) = (31.7 \pm 2.5)$ kJ·mol^{-1}. At low pulse repetition rates, the experimental k_p^{app} values are related to an averaged propagation rate coefficient, k_p^{av}, that is dependent on the relative population of chain-end and midchain radicals. Evaluated by comparing simulated and experimental molecular weight distributions, k_p^{av} provides an estimate for k_p^t. The Arrhenius parameters are: $A(k_p^t) = (1.52 \pm 0.14) \times 10^6$ L·mol^{-1}·s^{-1} and $E_a(k_p^t) = (28.9 \pm 3.2)$ kJ·mol^{-1}.

Introduction

The accuracy and reliability of free-radical propagation rate coefficients, k_p, has been considerably improved by application of the pulsed laser polymerization (PLP) size exclusion chromatography (SEC) technique.[1] The idea is found in earlier references,[2,3] but it was the development and experimental verification by Olaj et al.[1] that demonstrated the potential of the technique. A mixture of monomer and photoinitiator is illuminated by laser pulses separated by a time t_0, typically 0.01−0.2 s. Each pulse generates a burst of new radicals in the reaction mixture that will grow, provided that they escape termination, to a chain length L_0:[1,2]

$$L_0 = k_p[M]t_0 \quad (1)$$

with [M] being the monomer concentration. There is a high probability that the new radicals from the subsequent flash at t_0 will terminate these chains, such that a distinctive peak is formed in the polymer molecular weight distribution (MWD) corresponding to L_0, usually determined from the inflection point on the low-molecular-weight side of the peak.[1] Since radicals have a certain probability to survive the burst of termination at t_0 and to terminate at a later pulse, the relative concentration of polymer with chain lengths $L_1 = 2L_0$, $L_2 = 3L_0$, ..., is also increased. As a result, the technique produces a well-structured MWD with peaks at chain length L_0 and its multiples. Using eq 1 to determine k_p, the PLP−SEC technique has been applied successfully to many monomers.[4,5] Benchmark k_p values have been published by an IUPAC subcommittee on "Modeling of Polymerization Kinetics and Processes" for styrene,[6] several alkyl methacrylates,[7−9] and butyl acrylate.[10] The reliability of the k_p determination is validated by several consistency criteria,[7] among which the most important are that $L_1 = 2L_0$ (the chain length L_0 is used for determination of k_p, while L_1 is measured to check this consistency criterion) and that k_p values are independent from the initiator concentration, the pulse energy and the laser pulse repetition rate.

However, difficulties have appeared in the determination of k_p values for alkyl acrylates by the PLP−SEC technique at temperatures above 20 °C. For these monomers, molecular weight distributions (MWDs) obtained at 100 Hz (or less) and higher temperatures show either no structure or a broadened PLP structure.[10−22] Intramolecular transfer to polymer is now accepted as the mechanism responsible for this peak broadening,[10] a conclusion based on numerous experiments[23−31] and theoretical[32−34] considerations. In addition, the deviation of the stationary polymerization kinetics of alkyl acrylates from the behavior of other monomers[35−41] can also be attributed to intramolecular transfer to polymer.[35,42,43]

Intramolecular transfer to polymer, a mechanism often referred to as backbiting, generates a tertiary (midchain) radical, R^t, by abstraction of a hydrogen atom from an acrylate unit on the backbone of the secondary (chain-end) radical R^s, most likely via the formation of a six-membered ring, as shown in Scheme 1 for butyl acrylate (BA). Subsequent addition of monomer to R^t creates a short-chain branch (SCB) in the polymer and leads to re-formation of a chain-end radical. The propagation rate coefficient for monomer addition to the midchain radical, k_p^t, is significantly lower than addition to the secondary chain-end

* Corresponding author. E-mail: mbuback@gwdg.de. Fax: 49 551-39-31-44.
† Institute on Laser and Information Technologies.
‡ Department of Chemical Engineering, Dupuis Hall, Queen's University.
§ Institute for Physical Chemistry, University of Göttingen.

10.1021/ma071413o CCC: $37.00
Published on Web 11/03/2007

Scheme 1. Formation of a Midchain Tertiary Radical (R^t) by Intramolecular Chain Transfer of a Chain-End Secondary Radical (R^s), where Monomer Addition to the New Midchain Radical Structure Creates a Short-Chain Branch in the Polymer and Leads to Reformation of a Chain-End Radical

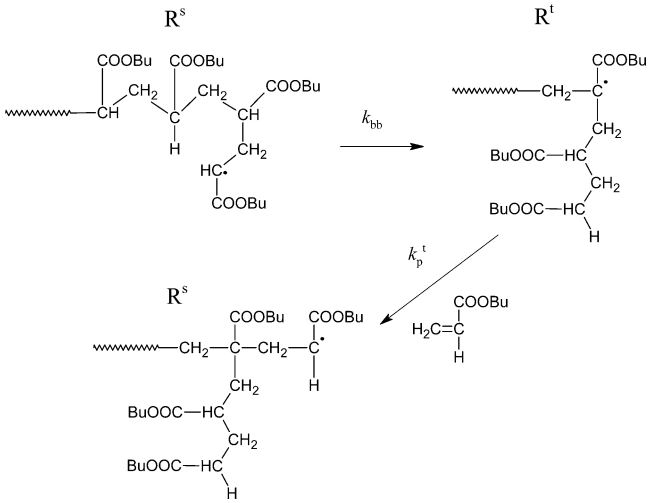

radical (denoted by k_p^s).[27,30,43] The relative concentrations of the two types of radicals can be estimated assuming that they achieve a dynamic equilibrium; i.e., making the quasi-steady state assumption on R^t:[42]

$$\frac{[R^t]}{[R^s]} = \frac{k_{bb}}{k_p^t[M] + k_t^{tt}[R^t] + k_t^{st}[R^s]} \tag{2}$$

In eq 2, k_{bb} is the backbiting rate coefficient, k_t^{tt} is the rate coefficient for termination of two midchain radicals, k_t^{st} is the rate coefficient for cross-termination of the two radical types, and other side reactions (i.e., β-scission of tertiary radicals) are assumed negligible. The rate of polymerization for the system is

$$R_p = (k_p^t[R^t] + k_p^s[R^s])[M] = (k_p^t x_{MCR} + k_p^s(1 - x_{MCR}))[M]([R^t] + [R^s]) = k_p^{av}[M]([R^t] + [R^s]) \tag{3}$$

where x_{MCR} (=$[R^t]/([R^t] + [R^s])$) is the fraction of midchain radicals. Equations 2 and 3 lead to the definition of an average propagation rate coefficient (or effective propagation rate coefficient) for the two-radical system, assuming that the probability of propagation is much higher than termination for midchain radicals ($k_p^t[M] \gg k_t^{tt}[R^t] + k_t^{st}[R^s]$ in eq 2, the so-called long-chain hypothesis):[27,42,44]

$$k_p^{av} = k_p^s - \frac{k_p^s - k_p^t}{1 + \dfrac{k_p^t[M]}{k_{bb}}} \tag{4}$$

which, as $k_p^t \ll k_p^s$, is transformed to

$$\frac{k_{bb}}{k_p^t} = [M]\left(\frac{k_p^s}{k_p^{av}} - 1\right) \tag{5}$$

It is also useful to remember that k_p^{av} is related to the fraction of midchain radicals in the system; from eq 3, $k_p^{av} = k_p^s(1 - x_{MCR})$ for $k_p^t \ll (k_p^s[R^s])/[R^t]$.

Some efforts have been made toward the evaluation of k_{bb} and k_p^t for butyl acrylate (BA). First, a measure of quaternary carbons via ^{13}C NMR has been used to determine k_{bb}, applying the expression for branching level (BL):[29]

$$BL = \frac{k_{bb}}{k_p^s[M] + k_{bb}} \tag{6}$$

The so-obtained Arrhenius parameters are: $E_a(k_{bb}) = 29.8$ kJ·mol^{-1} and $A(k_{bb}) = 4.31 \times 10^7$ s^{-1}.[29] (The values reported here are recalculated from the BL data in[29] using the IUPAC values[10] for k_p^s in eq 6.) The fraction of midchain radicals in the BA system has been measured by electron spin resonance spectroscopy (ESR) under PLP conditions by Willemse et al.,[30] with the difference in activation energies between backbiting and monomer addition to midchain radical estimated as $\Delta E_a = E_a(k_{bb}) - E_a(k_p^t) = 18.8$ kJ·mol^{-1}. This value is surprising, as it suggests, in conjunction with the above-mentioned value of $E_a(k_{bb}) = 29.8$ kJ·mol^{-1}, that the activation energy for monomer addition to midchain radicals, $E_a(k_p^t)$, is only 11 kJ·mol^{-1}, a value much lower than the 34 kJ·mol^{-1} measured for polymerization of the butyl acrylate dimer.[45] It could well be that the experimental conditions used in the ESR−PLP study do not allow the relative concentrations of R^s and R^t to reach an equilibrium ratio, especially at low temperatures, violating the quasi-steady-state assumption and/or long-chain hypothesis for midchain radicals and underestimating $E_a(k_p^t)$. Nonetheless, the work[30] provides an upper bound estimate of 68 L·mol^{-1}·s^{-1} for k_p^t at 50 °C, about 400 times lower than the value of k_p^s.[43]

In this work, we revisit the analysis of the MWDs produced by PLP−SEC to obtain estimates of both k_{bb} and k_p^t for BA. Simulations by Nikitin et al.[33,44] indicate that the PLP-generated MWDs yield valuable information, even if the growing radicals are subjected to backbiting events during the time between subsequent pulses. The apparent propagation rate coefficient (k_p^{app}, as measured from the first inflection point on the low-molecular-weight side of the MWD) varies with pulse repetition rate (PRR) between two limiting values. At high repetition rate, k_p^{app} provides a measure of the chain-end propagation rate coefficient (k_p^s), as the chains associated with the inflection point do not undergo any backbiting events between pulses.[10] As PRR is decreased, a greater fraction of chains undergo backbiting in the time between pulses; the slow reinitiation of these midchain radicals back to chain-end radicals by monomer addition (see Scheme 1) shifts the inflection point to a value lower than the expected position ($k_p^{app} < k_p^s$). As PRR is decreased even further, a chain has the opportunity to undergo several backbiting-reinitiation cycles in the dark time between pulses, such that k_p^{app} provides a measure of k_p^{av}, defined by eq 4. This approach has been experimentally explored by Castignolles[46] for BA polymerization initiated by pulsed UV lamp radiation at 15 °C, under which conditions k_p^{av} was estimated to be about 4800 L·mol^{-1}·s^{-1}. However, the k_p^{app} variation with repetition rate was found to be not reproducible, as the pulse energy of the lamp was not well stabilized. Thus, Castignolles recommended application of the PLP technique.

Very recently the variation in k_p^{app} with PLP repetition rate was reported for nonionized acrylic acid (AA) pulsed laser polymerization in the aqueous phase (9.6 wt % AA in water) at 6 °C,[47] and the data were used to estimate k_{bb}/k_p^t for AA under these conditions to be 2.4 mol·L^{-1}. The kinetics of AA polymerization in the aqueous system is complicated by the variation of k_p^s with acid concentration and degree of ioniza-

tion.[48,49] Therefore, we have returned to the BA system to investigate the feasibility of determining kinetic coefficients from the variation in k_p^{app} with PRR by PLP−SEC.

Experimental Part

Butyl acrylate (Fluka, 99% purity) is purified by passing through a column filled with inhibitor remover (Aldrich) to remove hydroquinone monomethyl ether, and is treated by several freeze-pump and thaw cycles to remove dissolved oxygen. DMPA (2,2-dimethoxy-2-phenylacetophenone, Aldrich, 99% purity) or MMMP (2-methyl-4-(methylthio)-2-morpholinopropiophenone, Aldrich, 98% purity) is added to the monomer at concentrations 5 to 16 mmol·L^{-1} under an argon atmosphere, and the mixture is transferred to a QS110 optical cell (Hellma-Worldwide) with a path length of 10 mm. The sample is maintained at the reaction temperature (−10, 0, +10, +20, and +30 °C) while being exposed to pulsed laser radiation for 10 to 50 pulses at 3−100 Hz and energies of 5−30 mJ per pulse to allow for about 0.5% monomer conversion to polymer; the LPX 210i excimer laser (Lambda Physics) of 20 ns pulse width was operated on the XeF line at 351 nm. Within one series of experiments in which laser pulse repetition rate is varied, the type and the concentration of initiator and laser pulse energy were the same, such that the concentration of radicals generated per pulse should remain constant. As the number of pulses and thus monomer conversion were low, no temperature increase in the cell was observed during pulsing. The reaction mixture after PLP was poured into a sample vial containing hydroquinone monomethyl ether (Fluka) in methanol to stop post-polymerization and precipitate the formed polymer. Residual monomer and methanol were evaporated by freeze drying under high vacuum.

The SEC analyses were performed at 35 °C with tetrahydrofuran as the eluent (1 mL·min^{-1} flow rate) on a system composed of a Waters HPLC pump (model 515), a JASCO AS-2055-plus autosampler, three PSS SDV columns (5 μm particle size; 10^5, 10^3, and 10^2 Å pore sizes) and a Waters refractive index detector (model 2410). The SEC setup was calibrated with polystyrene standards of narrow polydispersity (M_p = 410 to 2 000 000 g·mol^{-1}, PSS, Mainz, Germany). The obtained MWDs are recalculated according to the principle of universal calibration using Mark−Houwink parameters for linear polyBA ($K = 1.22 \times 10^{-2}$ mL·g^{-1}, a = 0.700).[14] Data acquisition and processing were carried out using the WinGPC software (PSS, Mainz, Germany).

Results and Discussion

Experiments at 20 °C. To confirm the dependence of k_p^{app} on PRR found by simulation,[44] PLP experiments have been carried out with BA at 20 °C, with laser repetition rate varied between 100 and 11 Hz. Experimental conditions were carefully selected for these (and all) experiments as follows:

- A low number of pulses were used to reduce broadening of the MWD due to initiator consumption (changes in initial radical concentration) and monomer conversion (changes in monomer concentration).
- A large sample volume was chosen to produce an amount of polymer sufficient for SEC analysis even at rather low monomer-to-polymer conversions.
- The reaction mixture was protected from ambient light to minimize formation of background non-PLP polymer.
- The optical setup was carefully aligned to minimize non-uniform irradiation of the sample cell.
- High initiator concentration and laser energy were used, to approach the high termination rate conditions[50] and to ensure chain-length control by laser pulsing.

The MWDs obtained in these experiments are shown in Figure 1a together with the associated first-derivative curves (Figure 1b). The features of the distributions and their derivative curves are in accord with the earlier experimental observations.[13,16] For the higher laser repetition rates (f = 100 and 62 Hz) the MWDs satisfy the main criterion of the PLP−SEC method for determining k_p^s: the second inflection point at chain length $L_1 \approx 2L_0$ is clearly observed in the first-derivative plots. Lowering of the PRR results in MWDs without clear PLP structure, due to the influence of intramolecular chain transfer.[10]

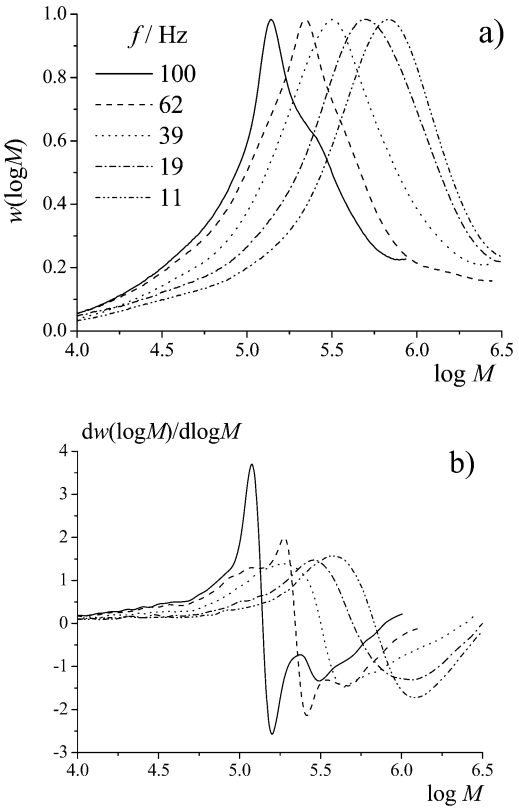

Figure 1. Experimental MWDs (a) and associated first-derivative curves (b) produced by PLP of butyl acrylate at 20 °C and different laser pulse repetition rates.

It is worthwhile expanding on the processes that control the PLP structure introduced earlier. The sharp peak observed in the MWDs generated at laser repetition rates of 100 and 62 Hz is the result of termination of secondary radicals that have survived the pulse separation time of t_0 (0.01 or 0.016 s). A fraction of the radicals undergoes intramolecular chain transfer to polymer during this time interval, as the characteristic time for backbiting is of the same order of magnitude as t_0; $\tau_{bb} = 1/k_{bb} = 0.005$ s, calculated using the Arrhenius parameters for k_{bb} from literature.[29] However, a sufficient fraction of radicals grow exclusively by chain-end propagation without undergoing backbiting during the period between pulses, thus producing a characteristic PLP structure at chain length L_0. Lowering PRR to 39 Hz and below, results in a greater fraction of radicals that undergo backbiting prior to the arrival of the subsequent laser pulse. As monomer addition to these midchain radicals is slow, the linear relationship between chain length and time (eq 1) is lost. Previous modeling work has indicated that a weak PLP structure may be maintained if the rate of monomer addition to the midchain radical (characteristic time $\tau_{MCR} = 1/(k_p^t[M])$) is fast relative to that of backbiting.[51] This is not observed in Figure 1: the MWDs are broadened and contain no PLP structure, thus violating the IUPAC consistency criteria for determination of propagation rate coefficients by the PLP−SEC method. Nevertheless, these MWDs should not be considered as meaningless; as they arise from termination of radicals subjected to backbiting events, they contain valuable information about rate coefficients

Table 1. Arrhenius Parameters for the Rate Coefficients Used for Simulation of Butyl Acrylate Polymerization

	pre-exponential factor, $L \cdot mol^{-1} s^{-1}$ or s^{-1}	activation energy, $kJ \cdot mol^{-1}$	reference
k_p^s	2.21×10^7	17.9	10
k_{bb}	4.84×10^7	31.7	this work
k_p^t	1.52×10^6	28.9	this work
$k_{tr,M}^s$	2.9×10^5	32.6	52
k_t^{ss}	1.34×10^9	5.6	5
k_t^{st}	2.74×10^8	5.6	this work, 5, 43
k_t^{tt}	1.8×10^7	5.6	this work, 5, 43
$k_{tr,M}^t$	2.0×10^5	46.1	52

associated with midchain radical formation (k_{bb}) and subsequent monomer addition (k_p^t).

Model of Acrylate Polymerization. The mechanistic model of acrylate polymerization at temperatures below 80 °C is given in Scheme 2. As the model is used to analyze low-conversion kinetic data, intermolecular chain transfer to polymer is not included, nor is β-scission of tertiary radicals since the mechanism has been found to be of negligible importance in this temperature regime.[27,28] The added complexity of chain-length dependent (CLD) termination is not considered; CLD termination has negligible effect on the position and breadth of the main MWD peak which is controlled by termination of radicals with lifetime t_0 with newly generated short radicals. The different reactivity of midchain (R_i^t) and chain-end (R_i^s) radicals in propagation and termination mechanisms is explicitly considered, and termination is assumed to take place exclusively by combination.

Scheme 2. Acrylate Polymerization Mechanism

initial propagation step	$R_0 + M \xrightarrow{k_i} R_1^s$	(i)
propagation	$R_i^s + M \xrightarrow{k_p^s} R_{i+1}^s$	(ii)
backbiting	$R_i^s \xrightarrow{k_{bb}} R_i^t$	(iii)
addition to midchain radical	$R_i^t + M \xrightarrow{k_p^t} R_{i+1}^s$ (+SCB)	(iv)
chain transfer to monomer	$R_i^s + M \xrightarrow{k_{tr,M}^s} P_i + R_1^s$	(v)
	$R_i^t + M \xrightarrow{k_{tr,M}^t} P_i + R_1^s$	(vi)
termination by combination	$R_i^s + R_j^s \xrightarrow{k_t^{ss}} P_{i+j}$	(vii)
	$R_i^t + R_j^t \xrightarrow{k_t^{tt}} P_{i+j}$	(viii)
	$R_i^s + R_j^t \xrightarrow{k_t^{st}} P_{i+j}$	(ix)

Table 1 contains the frequency factors and activation energies of the rate coefficients for the reactions given in Scheme 2. The Arrhenius parameters for the rate coefficients of backbiting and addition to midchain radical are determined in this work, as presented later. The activation energies for the termination rate coefficients k_t^{ss}, k_t^{tt} and k_t^{st} are chosen to be the same as in ref 5, and the pre-exponential factors are calculated from the lumped rate coefficients $k_t^{ss}/(k_p^s)^2$, $\theta_1 = (2k_t^{st}k_{bb})/(k_t^{ss}k_p^t)$, and $\theta_2 = (k_t^{tt}/k_t^{ss})(k_{bb}/k_p^t)^2$ reported in ref 43 from analysis of experimental rate data at 50 °C based upon the mechanistic set of Scheme 2.

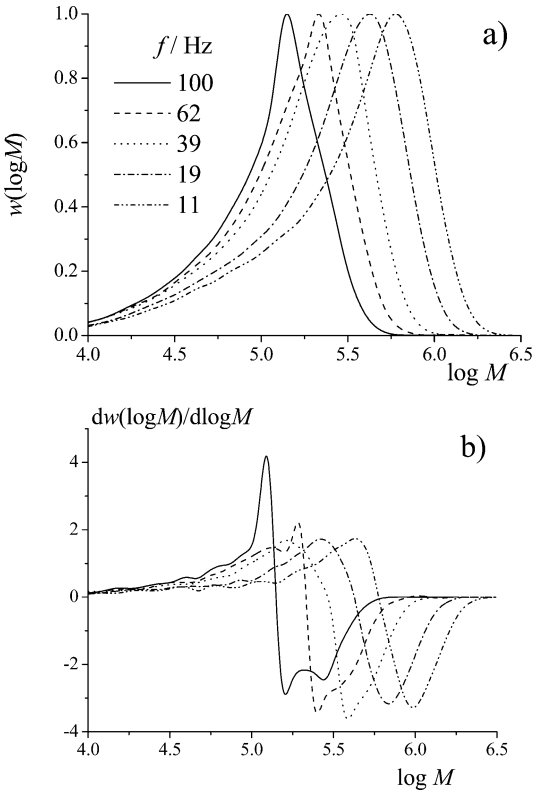

Figure 2. Simulated MWDs (a) and associated first-derivative curves (b) produced by PLP of butyl acrylate at 20 °C and different laser pulse repetition rates, *f*. Calculated for [M] = 7.02 mol·L^{-1}, [R_0] = 6.5×10^{-6} mol·L^{-1}, and $b\sigma = 0.04$. Other rate coefficients are chosen according to Table 1.

The model of butyl acrylate polymerization is implemented using the simulation program PREDICI (polyreaction distributions by countable system integration),[53] version 6.22p.academic, on an Intel Celeron 1.8 GHz computer. MWDs are calculated for pseudostationary conditions, by considering only the polymer produced after the initial transient period has passed (generally less than five pulses). SEC broadening of the calculated MWD is introduced according to the procedure described in ref 54.

Figure 2 presents the MWDs calculated for BA polymerization at 20 °C, with PRRs, *f*, chosen to be the same as for experiments given in Figure 1 and rate coefficients as specified in Table 1. The additional parameters required for simulation are the concentration of radicals produced per laser pulse, [R_0] = 6.5×10^{-6} mol·L^{-1}, and the dispersion parameter used to represent SEC broadening of the MWD, $b\sigma = 0.04$. The evaluation of these parameters is described below. The calculated distributions in Figure 2 capture the features of the experimental distributions and their first-derivative curves very well. As observed experimentally, the simulated distributions exhibit no PLP structure at repetition rates of 39 Hz and below. At the same time, these distributions still shift to higher MWs with the increase of pulse separation time since the position of the peak is controlled by the burst of radical termination occurring at t_0. The peak provides a measure of the apparent propagation rate coefficient, k_p^{app}, evaluated by applying the standard PLP−SEC methodology (i.e., by using the inflection point on the low-molecular weight side of the peak to determine k_p^{app}). This paper outlines the procedure by which the variation of k_p^{app} with PRR is used to estimate k_{bb} and k_p^t. It is first demonstrated using simulated distributions (with known input rate coefficients), and is then applied to the analysis of the experimental MWDs.

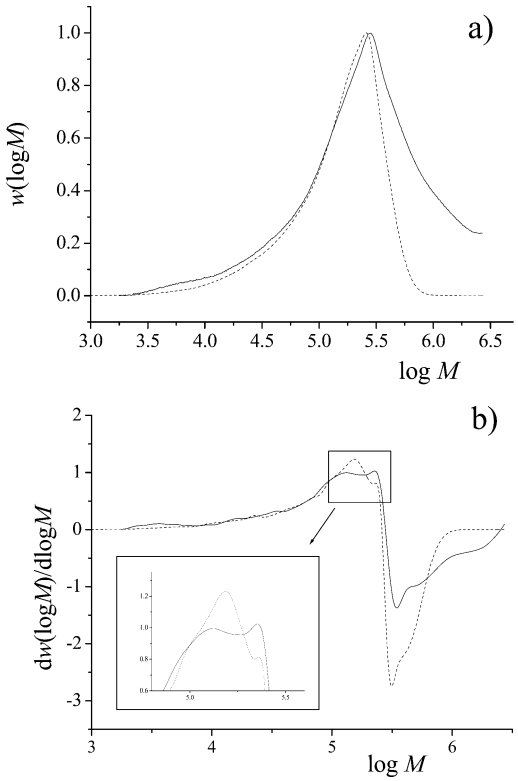

Figure 3. Experimental (solid line) and simulated (dashed line) MWDs (a) and associated first- derivative curves (b) produced by PLP of butyl acrylate at 20 °C at a laser repetition rate 49 Hz. Simulated MWD has been calculated for [M] = 7.02 mol·L^{-1}, [R_0] = 6.5 × 10^{-6} mol·L^{-1}, and $b\sigma$ = 0.04. The other rate coefficients are chosen according to Table 1.

Method Development

Before discussing how k_p^{app} is related to other kinetic coefficients, it is important to first discuss how it is determined from the measured MWDs. Close examination of Figures 1 and 2 reveals that the first-derivative curve obtained at 62 Hz contains a broader maximum followed by a sharper peak. Another example is shown in Figure 3, where both experimental and simulated MWDs of BA polymerization at 20 °C with a pulse repetition rate of 49 Hz show two peaks in the first derivative curves. One arises from the termination of radicals that have undergone backbiting and the other comes from termination of secondary radicals that have escaped backbiting. These two peaks are easily distinguished: the peak formed from the radicals that have delayed growth due to a backbiting event is located at lower MW; this peak is also considerably broader than the other, as it is made up of the population of chains that have undergone multiple kinetic events of different time scales—chain-end radical propagation, backbiting, and (perhaps) mid-chain radical propagation. The sharper peak at higher MW results from termination of the radicals that have grown without undergoing backbiting, and is used to calculate the value of k_p^{app}. This situation only occurs at intermediate PRR; higher PRRs give distributions that have a sharper primary inflection point (and sometimes also a secondary inflection point), and lower PRRs give distributions with broader first-derivative curves having a single inflection point.

Using this approach, the variation of k_p^{app} with repetition rate for BA polymerization at 20 °C has been evaluated from simulated MWDs. The results presented in Figure 4 are calculated for two concentrations of laser-produced primary radicals per pulse, [R_0] = 1.0 × 10^{-6} and 1.0 × 10^{-5} mol·L^{-1},

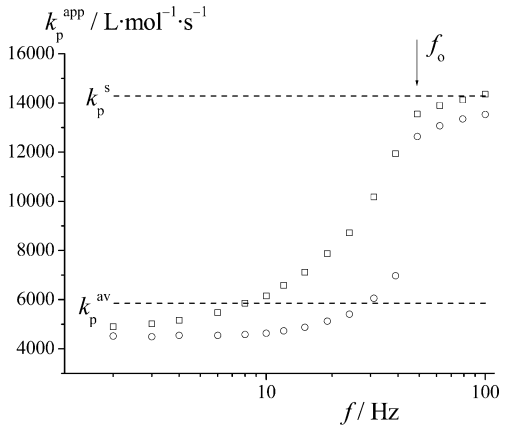

Figure 4. Variation of apparent propagation rate coefficient, k_p^{app}, with laser pulse repetition rate, f, simulated for PLP of butyl acrylate at 20 °C. The MWDs have been calculated for [M] = 7.02 mol·L^{-1}, $b\sigma$ = 0.04, [R_0] = 1.0 × 10^{-6} (□) and 1.0 × 10^{-5} (○) mol·L^{-1}. The other rate coefficients are chosen according to Table 1. Horizontal dashed lines indicate the input values of k_p^s (upper) and k_p^{av} (lower).

with the other rate coefficients as given in Table 1. The values of k_p^{app} vary between two limiting values that are relatively insensitive to the input value of [R_0]. At high repetition rates, k_p^{app} is close to the input value for the propagation rate coefficient of secondary radicals, k_p^s. This result is expected, as the peak is formed by the termination of secondary radicals that have not been subjected to backbiting. The slight offset between k_p^{app} and the input value of k_p^s for [R_0] = 1.0 × 10^{-5} mol·L^{-1} is because the system is approaching the high termination limit, where the MWD peak position is a better measure of L_0 than the point of inflection, as discussed elsewhere.[50] At low repetition rates, k_p^{app} approaches a constant value that is close to k_p^{av}, as calculated by eq 4. Between these two plateau values, k_p^{app} decreases with decreasing repetition rate according to a sigmoidal shape, with the steepness of the decline being affected by the concentration of radicals generated per pulse. The repetition rate at which a sharp decrease in k_p^{app} is observed as PRR is lowered is denoted by f_o; this repetition rate is also the last at which the sharp peak in the first-derivative curve associated with k_p^s is observable. The features of the curve in Figure 4 provide the basis for the procedures for evaluating individual rate coefficients.

Evaluation of k_{bb}. The decrease of pulse repetition rate results in a broadening of the PLP-generated MWD as the fraction of chains that undergoes intramolecular chain transfer increases, and a sharp decrease in k_p^{app} occurs at f_o. According to reaction iii in Scheme 2, the fraction of radicals that are not subjected to backbiting is proportional to exp(−$k_{bb}t$), where t is the time after generation of these radicals by a laser pulse. If this fraction is too low (PRR less than f_o), an insufficient population of polymer molecules are formed to produce a sharp peak in MWD (and in the first-derivative plot). The lowest fraction, x_{min}, of secondary radicals (with respect to total radical concentration at time $t = 1/f_o$) that still allows for the observation of the sharp peak in the first-derivative curve associated with k_p^s can be assumed to be independent of the particular polymerization conditions, x_{min} = exp(−k_{bb}/f_o) = const. The simulation results shown in Figure 4 indicate that f_o is indeed not sensitive to [R_0], such that it is possible to conclude that k_{bb} is directly proportional to f_o:

$$k_{bb} = a_p f_o \qquad (7)$$

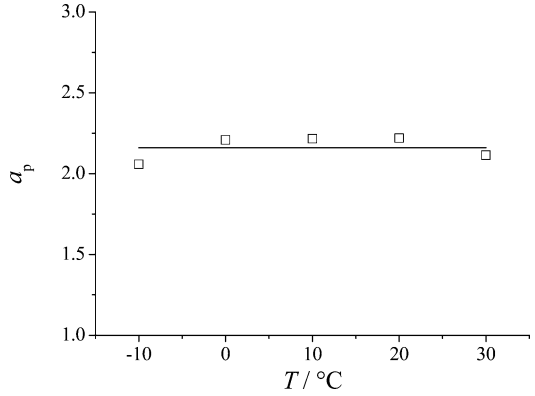

Figure 5. Proportionality constant a_p determined for different temperatures according to eq 7, with values of f_o determined from simulated MWDs for BA polymerization at different pulse repetition rates using the model given in Scheme 2 and rate coefficients in Table 1, with $[R_0] = 1.0 \times 10^{-5}$ mol·L^{-1} and $b\sigma = 0.04$.

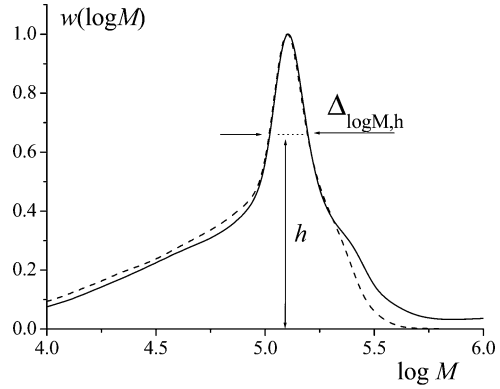

Figure 6. Experimental (solid line) and simulated (dashed line) MWDs for PLP of butyl acrylate at −10 °C and a laser pulse repetition rate 49 Hz. Simulated MWD has been calculated for [M] = 7.26 mol·L^{-1}, $[R_0] = 1.0 \times 10^{-5}$ mol·L^{-1} and $b\sigma = 0.049$. Other rate coefficients are chosen according to Table 1.

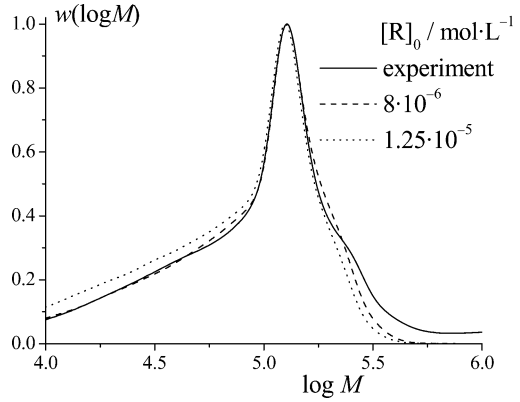

Figure 7. Experimental (solid line) and simulated (dashed and dotted lines) MWDs for PLP of butyl acrylate at −10 °C and a laser repetition rate of 49 Hz. Simulated MWD has been calculated for [M] = 7.26 mol·L^{-1}, $b\sigma = 0.049$ and $[R_0]$ as indicated. The other rate coefficients are chosen according to Table 1.

This expression can be used to determine the absolute value of k_{bb} from the dependency of k_p^{app} on repetition rate, provided that the value of the proportionality constant a_p that relates k_{bb} to f_o may be determined. In Figure 4, for example, the input value for k_{bb} is 109 s^{-1} and the critical repetition rate is 49 Hz; thus the value of a_p is evaluated to be 2.22.

To confirm the validity of eq 7, values of f_o have been evaluated by simulation from distributions calculated at different temperatures using the model outlined above. The corresponding values of a_p determined according to eq 7 are shown in Figure 5, with the values of k_{bb} calculated according to the Arrhenius dependence in Table 1. The value of a_p is indeed seen to be constant, with a value of 2.16 ± 0.03. Further simulations indicate that the value is dependent on the amount of SEC broadening that occurs; for the same input value of k_{bb}, f_o shifts to a lower value as the broadening parameter $b\sigma$ is decreased (and the MWDs become sharper), such that the value of the proportionality constant a_p increases. Therefore, the value of $b\sigma$ must be determined experimentally in order to relate f_o to k_{bb}.

Evaluation of k_p^{av} and k_p^t. It is seen in Figure 4 that, although the values of k_p^{app} at low PRR approach a constant value close to the simulation input value for k_p^{av}, there is an offset by as much as 30%. At these lower repetition rates, a larger fraction of the radicals terminate before the next pulse arrives, compared to the system at high PRR. This increases the relative offset between k_p^{app} and k_p^{av} compared to that between k_p^{app} and k_p^s. In addition, the peak formed from termination of radicals that are subjected to backbiting is broader compared with the peak formed as a result of termination of secondary radicals that have escaped intramolecular transfer to polymer. Thus, the associated inflection point from the first derivative curve systematically underpredicts k_p^{av}. The magnitude of the offset depends on the value of the initial radical concentration produced by a pulse, $[R_0]$, and on the extent of broadening. An iterative approach has been developed to estimate k_p^{av} (and thus k_p^t), as will be detailed with the experimental results. First, however, the estimation of $b\sigma$ and $[R_0]$ is presented.

Evaluation of $b\sigma$ and $[R_0]$. MWDs generated by PLP can exhibit broadening for numerous reasons. Many of them are related to experimental conditions during pulsing: radical concentrations may vary spatially or with the number of pulses because of initiator consumption, laser attenuation, nonuniform irradiation, and/or inhibition.[55] As mentioned previously, every attempt was made to minimize these experimental broadening effects. In addition, natural broadening occurs due to the stochastic nature of free-radical polymerization, and also results from dispersion effects during MW separation in the SEC columns. As can be seen in Figures 1 and 2, the narrowest MWD peaks are obtained (both experimentally and via simulation) at higher laser repetition rates. Thus, it is these distributions that are selected for estimating the value of $b\sigma$. The width $\Delta_{\log M,h}$ of the peak at some height $h < h_{max}$, where h_{max} is the maximum height of the peak, is considered. This value of h should be selected large enough such that $\Delta_{\log M,h}$ is measured for the narrow peak associated with the termination of chain-end radicals controlled by the laser repetition rate, as this width is mainly dependent on Poisson broadening, kinetic broadening (due to termination not occurring instantaneously at t_0), and instrumental broadening. The value of $b\sigma$ is then estimated by obtaining the best match between the experimental and simulated widths $\Delta_{\log M,h}$, as illustrated in Figures 6 and 7 for BA pulsed at 49 Hz and −10 °C. The measured and simulated (with dispersion parameter $b\sigma = 0.049$) MWDs are normalized such that the ordinates of the peak maxima for both distributions are equal to unity. Within one series of experiments carried out at the same initiator concentration and pulse energy, the values of $b\sigma$ estimated for different distributions are close to each other. In addition, the value is not particularly sensitive to the choice of h; the value of $b\sigma$ changes only from 0.048 to 0.050 as h is decreased from 0.95 to 0.55.

The sharp MWD peak results from termination of secondary radicals and thus is also influenced by the rate of termination, in particular by short−long termination. The termination rate coefficients k_t^{ss}, k_t^{tt}, and k_t^{st} values are assumed known according to Table 1; only the value for $[R_0]$ must be estimated in order to characterize the termination event fully. In addition, the determination of $[R_0]$ is important for the procedure used to evaluate k_p^{av} and k_p^t values. The fitting of experimental MWDs to estimate rate coefficients is well established. Moad et al.[56] were the first to use the MWDs produced by PLP to estimate k_t with known values of $[R_0]$. Here we do the opposite, using the experimental MWDs to estimate $[R_0]$ assuming that the values of k_t^{ss}, k_t^{tt}, and k_t^{st} are known. The mode of termination is chosen to be predominantly by combination in accordance with the literature[46] and also with the recent observation that the distribution immediately before and after the termination-controlled peak have similar heights for PLP-generated MWDs obtained at conditions close to the high termination rate limit when termination occurs predominately by combination.[57] Figure 6 presents the result of fitting of the measured MWD. According to this simulation the best value of $[R_0]$ is found to be 1.0×10^{-5} mol·L^{-1}. MWDs calculated for $[R_0] = 8.0 \times 10^{-6}$ and 1.25×10^{-5} mol·L^{-1} are compared to the same experimental MWD in Figure 7. Though the distribution of macromolecules before the peak is well fitted for the MWD calculated using $[R_0] = 8.0 \times 10^{-6}$ mol·L^{-1}, the shoulder after the peak deviates clearly from the one in the experimental MWD. The distribution before the peak for MWD calculated with $[R_0] = 1.25 \times 10^{-5}$ mol·L^{-1} deviates considerably from the one in the experiment. Therefore, the intermediate value $[R_0] = 1.0 \times 10^{-5}$ mol·L^{-1} (Figure 6) is chosen as the best value to reproduce the experimental MWD. Note that the estimate of the peak width ($\Delta_{\log M,h}$) and thus $b\sigma$ are relatively insensitive to $[R_0]$, such that both parameters can be determined simultaneously from fitting.

Analysis of Experimental MWDs. The measured dependencies of k_p^{app} on PRR for butyl acrylate at temperatures of −10, 0, +10, +20, and +30 °C are presented in Figure 8. At temperatures of 10 and 30 °C, the results of two series of PLP experiments are shown. The horizontal dashed lines in each plot indicate the input values of k_p^s (based upon the IUPAC expression of Table 1) and k_p^{av} (calculated using eq 4 with the Arrhenius parameters for k_{bb} and k_p^t estimated in this work).

The k_p^{app} values obtained at high repetition rates are slightly lower, but still within 20%, of the IUPAC k_p^s values. This difference is also seen in the simulation results shown as Figure 4 for $[R_0] = 1.0 \times 10^{-5}$ mol·L^{-1}. Under these high termination rate limit conditions, it has been shown that the inflection point can underestimate the true experimental value.[50] At 0 °C, a lower value of $[R_0]$, 3.0×10^{-6} mol·L^{-1}, is estimated, and the measured k_p^{app} value is in excellent agreement with the IUPAC k_p^s value.

Table 2 summarizes the final set of parameters and rate coefficients estimated from data at each temperature. Recall that the reported values for f_o are proportional to k_{bb}, with the proportionality constant being dependent on SEC broadening. For the distributions between 0 and 30 °C, $b\sigma$ is found to be close to the value of 0.04, resulting in an estimate for a_p of 2.16 according to simulation. At −10 °C, the distributions are well fit with $b\sigma = 0.051$, and an a_p value of 1.67 is estimated. Thus, k_{bb} values have been estimated at each temperature according to eq 7. Linear least-squares fitting of the Arrhenius relation $\ln(k_{bb}) = \ln A - E_a/RT$ to these values for the temperature range of −10 to +30 °C results in eq 8.

$$\ln(k_{bb}/s^{-1}) = 17.7 - 3812T^{-1}/K^{-1} \quad (8)$$

The Arrhenius plot is shown in Figure 9. The associated values of pre-exponential factor and activation energy are $A = (4.84 \pm 0.29) \times 10^7$ s^{-1} and $E_a = (31.7 \pm 2.5)$ kJ·mol^{-1}, respectively.

The remaining task is to estimate k_p^{av} (and thus k_p^t) from the limiting values of k_p^{app} found at low pulse repetition rates. This has been accomplished as follows:

(i) According to the simulation results of Figure 4, the values for k_p^{av} are expected to be higher than k_p^{app} at low repetition rates. An initial guess for k_p^{av} is made based upon the experimental results in Figure 8. The values 2600, 3700, 4700, 5600, and 6850 L·mol^{-1}·s^{-1} have been chosen at temperatures −10, 0, +10, +20, and +30 °C, respectively.

(ii) Assuming $b\sigma = 0.04$, initial values of k_{bb} are estimated from the experimentally determined values of f_0 at each temperature.

(iii) eq 5 is then used to evaluate k_p^t values. These first estimates for k_{bb} and k_p^t are used to calculate the termination rate coefficients according the procedure outlined above (these coefficients were practically the same as the ones in Table 1) and to simulate the MWDs using the model. Values of $b\sigma$ and $[R_0]$ are estimated for each series of experiments by fitting simulated distributions to the MWDs measured at high repetition rates, as described above.

(iv) These values for $b\sigma$ and $[R_0]$ are used to update the k_{bb} estimates; eq 8 reports the final Arrhenius parameters for k_{bb} determined after convergence of this procedure.

(v) The estimate for k_p^{av} at each temperature is updated by simulating MWDs obtained at low laser pulse repetition rates, using the predetermined values of $b\sigma$ and $[R_0]$. The aim of these simulations is to determine the difference Δ_{av} between the input value of k_p^{av} and the value of k_p^{app} for the lowest repetition rates examined experimentally, as illustrated in Figure 10a for the set of experiments at −10 °C; $k_p^{th,0}$ represents the value of k_p^{app} determined from the simulated MWDs. The difference has been calculated for five repetition rates; at the lowest value (3 Hz) Δ_{av} is estimated to be 655 L·mol^{-1}·s^{-1}, and the variation in k_p^{app} with repetition rate is well described by an exponential function in which a, b, and c are constants:

$$k_p^{app} = a + b \times \exp(cf/Hz) \quad (9)$$

(vi) Equation 9 is also suitable to describe the difference between k_p^{app} and k_p^{av} for the experimental data. The nonlinear least-squares fitting of the experimental points at −10 °C by eq 9 results in k_p^{app} (L·mol^{-1}·s^{-1}) = 1802 + 152.3 × exp(0.206f/Hz), with the fit to the data also shown in Figure 10b. At the lowest pulse repetition rate of 3 Hz, the apparent propagation rate coefficient is equal to 2084 L·mol^{-1}·s^{-1}. Therefore, the corrected value for k_p^{av} is calculated as ($k_p^{exp,0} + \Delta_{av}$) = 2739 L·mol^{-1}·s^{-1}.

It should be stressed that this final estimated value for k_p^{av} does not differ greatly from the initial guess of 2600 L·mol^{-1}·s^{-1}. The same was found at all temperatures: the preliminary values estimated for k_{bb} and k_p^{av} (and thus k_p^t by eq 5) were within 5% of the final converged values in all cases. Therefore, there was no need to reestimate the values of $b\sigma$ and $[R_0]$ (determined using the initial guesses for k_{bb} and k_p^t).

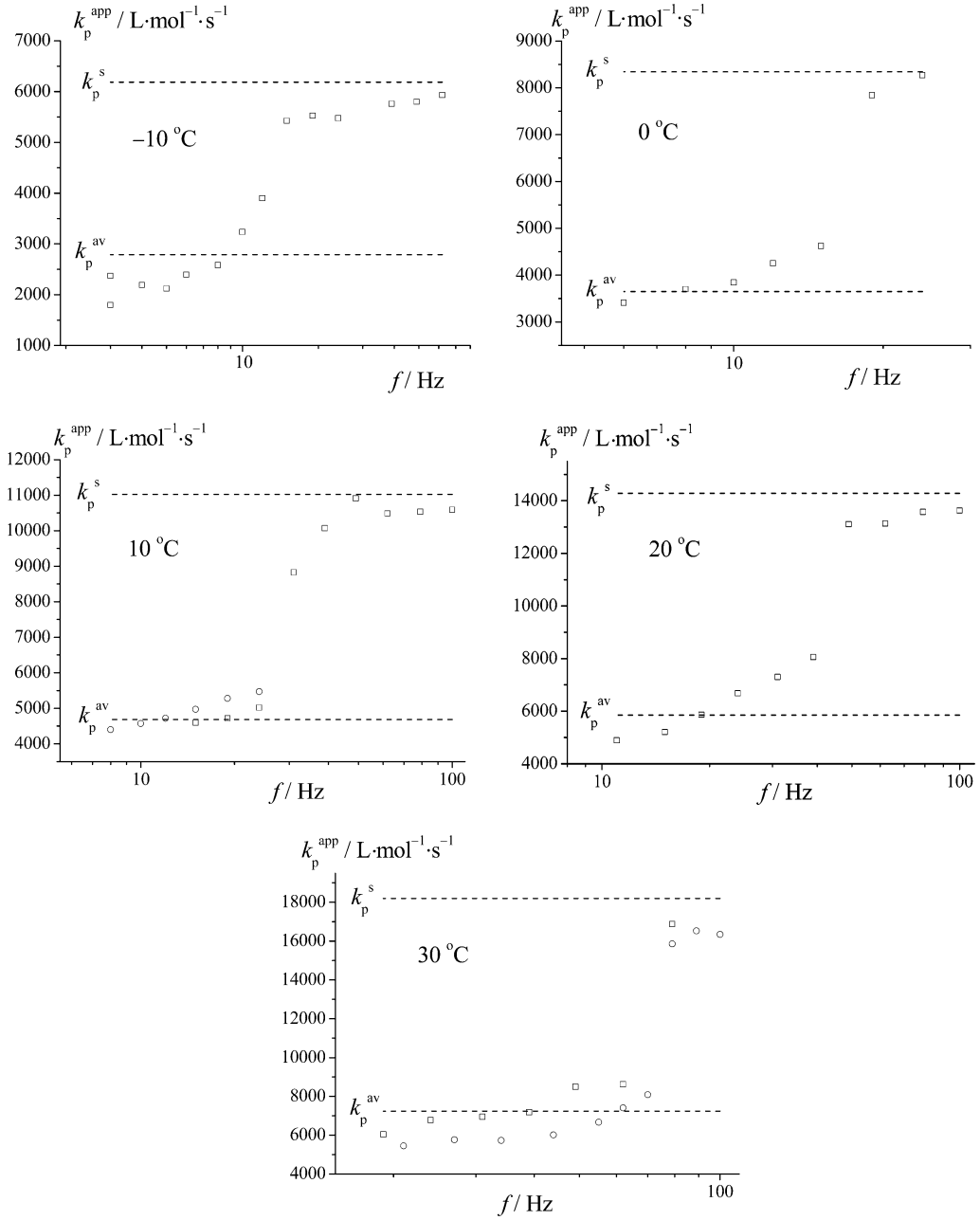

Figure 8. Dependency of apparent propagation rate coefficient, k_p^{app}, on pulse repetition rate, f, obtained by PLP−SEC experiments for butyl acrylate at −10, 0, +10, +20, and +30 °C. At temperatures of 10 and 30 °C, the results of two series of experiments are shown, by squares and circles. The horizontal dashed lines indicate the IUPAC value of k_p^s and the estimated value of k_p^{av} (determined on the basis of the Arrhenius parameters for k_{bb} and k_p^t obtained in this work), respectively.

The final estimates for k_p^{av} at each temperature are used to evaluate k_p^t according to eq 5 and are summarized in Table 2. These values are fitted by the Arrhenius relation, according to

$$\ln(k_p^t/\text{L·mol}^{-1}\text{·s}^{-1}) = 14.23 - 3475T^{-1}/\text{K}^{-1} \qquad (10)$$

The Arrhenius plot is shown in Figure 11. The associated values of pre-exponential factor and activation energy are $A = (1.52 \pm 0.14) \times 10^6$ L·mol^{-1}·s^{-1} and $E_a = (28.9 \pm 3.2)$ kJ·mol^{-1}, respectively.

Comparison of k_{bb} and k_p^t Estimates with Literature Data. The Arrhenius parameters for k_{bb} obtained in our work ($E_a = 31.7$ kJ·mol^{-1} and $A = 4.84 \times 10^7$ s^{-1}) for butyl acrylate polymerization are not significantly different from the ones determined by Plessis et al.[29] ($E_a = 29.8$ kJ·mol^{-1} and $A = 4.31 \times 10^7$ s^{-1}) via ^{13}C NMR analysis of quaternary carbon atoms. Because of the minor difference in activation energy, the k_{bb} values of the present work are by about a factor of 2 below the ones reported from Plessis et al. (see Figure 9). Although the experimental data in ref 29 provide a more direct measure of k_{bb}, the NMR signal-to-noise ratio may cause an appreciable scatter of the data, as can be seen from Figure 9. Interestingly, the k_{bb} data from the two independent experiments appears to be in closer agreement at the higher temperatures (see Figure 9), where the S/N ratio of the NMR measurements should be higher because of a larger content of quaternary carbon atoms. It should further be noted that the variation of k_p^{app} with pulse repetition rate, in particular the strong decrease at the repetition rate f_o, as observed in our experiments, may not be simulated via the literature k_{bb} data. Furthermore, the Plessis et al. k_{bb} data cannot represent the sharp PLP peak found in BA polymerization experiments at 60 °C using a pulse

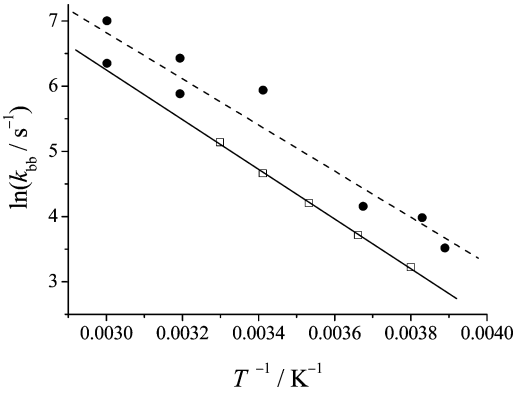

Figure 9. Arrhenius plot of backbiting rate coefficient (k_{bb}) for butyl acrylate. The solid line represents the best fit of experimental data obtained in this work (□) by eq 8. The dashed line represents the best fit of experimental data (●) taken from ref 29.

Table 2. Values of Parameters and Rate Coefficients Estimated from the Experimental Dependency of Apparent Propagation Rate Coefficient on Pulse Repetition Rate Measured by PLP−SEC for Butyl Acrylate

T, °C	$b\sigma$	$[R_0]$, mol·L^{-1}	f_o, Hz	a_p	k_{bb}, s^{-1}	k_p^{av}, L·mol^{-1}·s^{-1}	k_p^t, L·mol^{-1}·s^{-1}
−10	0.051	1.0×10^{-5}	15	1.67	25.1	2739	2.7
0	0.039	3.0×10^{-6}	19	2.16	41.0	3727	4.7
10	0.040	7.0×10^{-6}	31	2.16	67.0	4776	7.3
		3.5×10^{-6} [a]					
20	0.040	6.5×10^{-6}	49	2.16	105.8	5802	10.6
30	0.040	1.0×10^{-5}	79	2.16	170.6	7193	15.9
		2.5×10^{-5} [a]					

[a] For the data set shown by circles in Figure 8

repetition rate of 200 Hz.[21] Simulation via the Arrhenius parameters obtained in this work, on the other hand, are able to predict this peak. Despite these minor differences, the agreement between the literature k_{bb} values and the ones from the present study must be considered to be satisfactory.

With this work, we also provide an estimate for the rate of monomer addition to midchain radical (k_p^t) and its variation with temperature, best described by an activation energy of 28.9 kJ·mol^{-1}. This value differs substantially from the activation energy that can be inferred from the PLP−ESR results reported by Willemse et al.[30] However, as discussed in the Introduction, it is likely that radical stationarity is not achieved under their experimental conditions. An upper bound of k_p^t may be estimated by examining BA addition to a butyl methacrylate (BMA) radical. While located on a tertiary carbon, this radical is not as hindered as the midchain radical that results from backbiting (compare Scheme 3a with Scheme 1). An approximate limiting value is estimated via the simplifying terminal model approach for copolymerization as follows:

$$k_{p,upper}^t/\text{L·mol}^{-1}\text{·s}^{-1} = \frac{k_{p,BMA}}{r_{BMA,BA}} \qquad (11)$$

where $r_{BMA,BA}$ is the reactivity ratio for relative addition rate coefficients of BMA and BA to the BMA radical, and $k_{p,BMA}$ is the BMA homopropagation rate coefficient. As has been shown recently,[58] the terminal model may be used for deducing approximate k_p values for acrylate−methacrylate copolymerizations with the two monomers having the same type of alkyl ester moiety. The IUPAC-recommended Arrhenius coefficients[8] for the latter are $A(k_{p,BMA}) = 3.78 \times 10^6$ L·mol^{-1}·s^{-1} and E_a-

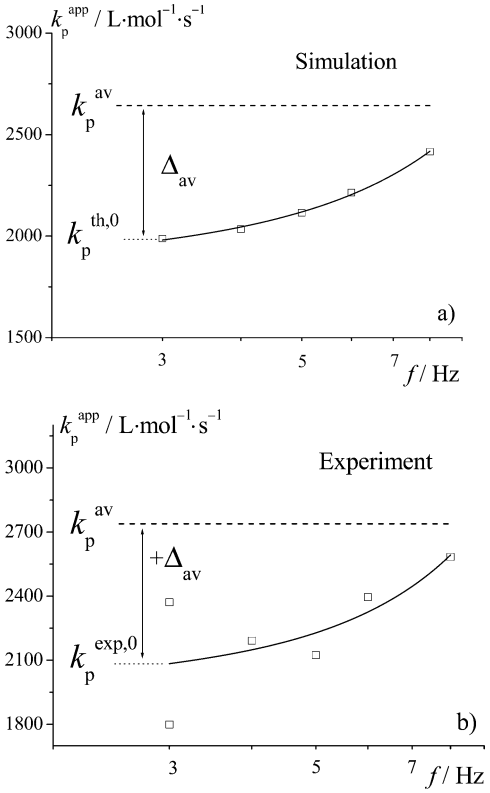

Figure 10. Methodology for evaluation of k_p^{av} by considering the variation in k_p^{app} with repetition rate for $f < 10$ Hz, illustrated for PLP−SEC experiments for butyl acrylate at −10 °C. The lines indicate the best fit of the simulated (top) and experimental (bottom) data using an exponential function, as described in the text.

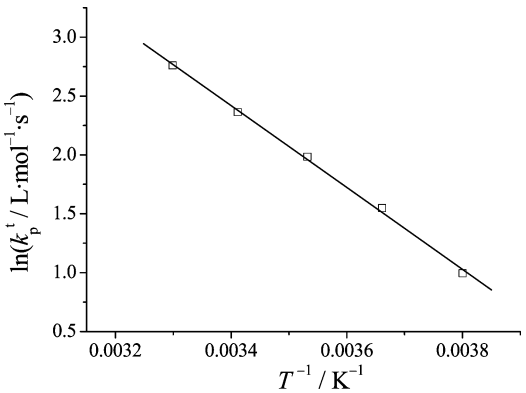

Figure 11. Arrhenius plot of rate coefficient, k_p^t, for the addition of butyl acrylate to the midchain radical formed by backbiting. The line represents the best fit of experimental data by eq 10.

($k_{p,BMA}$) = 22.9 kJ·mol^{-1}; and the reactivity ratio is taken from literature as

$$r_{BMA,BA} = 0.827 \exp(282.1T^{-1}/\text{K}^{-1}) \qquad (12)$$

The latter expression is from a study of BA copolymerization with methyl methacrylate,[59] but was found to provide a good representation of the BMA-BA system.[60] Thus:

$$k_{p,upper}^t/\text{ L·mol}^{-1}\text{·s}^{-1} = 4.6 \times 10^6 \exp(-3036T^{-1}/\text{K}^{-1}) \qquad (13)$$

which corresponds to an activation energy of 25.2 kJ·mol^{-1} and a value of 145 L·mol^{-1}·s^{-1} for $k_{p,upper}^t$ at 20 °C.

The midchain radical structure of BA is similar to that formed by polymerization of BA dimer. Thus, the polymerization

Scheme 3. Reactions That Provide Bounding Estimates for Butyl Acrylate Addition to an Acrylate Midchain Radical (Shown as Scheme 1): (a) Butyl Acrylate Addition to a Butyl Methacrylate Radical; (b) Butyl Acrylate Dimer Addition to the Associated Midchain Radical[a]

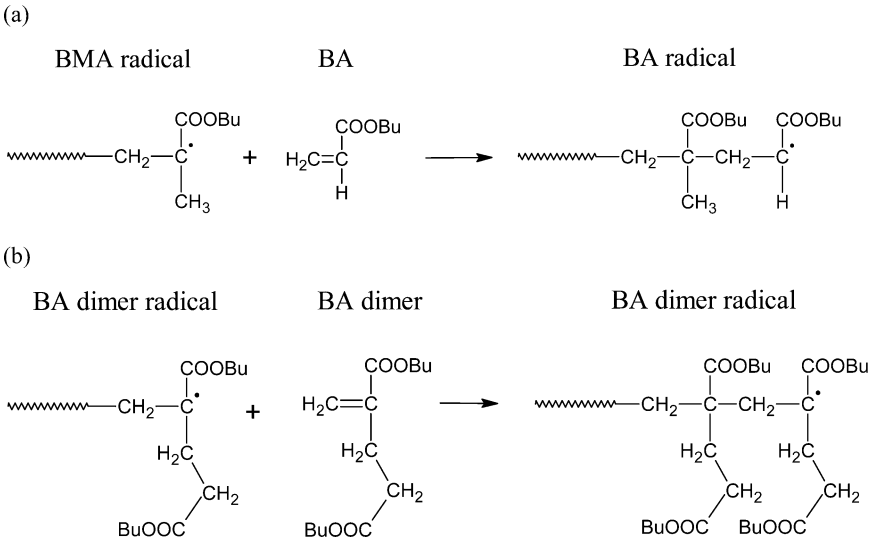

[a] See text for further discussion.

behavior of the dimer species provides a lower bound estimate for k_p^t; although the radical structure is similar, the addition of bulky BA dimer to the radical may be hindered compared to addition of BA monomer (compare Scheme 3b to Scheme 1). Müller studied the propagation of BA dimer using the PLP−SEC technique and fitted the following Arrhenius expression to the data:[45]

$$k_{p,lower}^t / \text{L·mol}^{-1}\text{·s}^{-1} = k_{p,dimer}/\text{L·mol}^{-1}\text{·s}^{-1} = 9.31 \times 10^6 \exp(-4065 \cdot T^{-1}/\text{K}^{-1}) \quad (14)$$

This corresponds to an activation energy of 33.8 kJ·mol^{-1} and a value of 8.8 L·mol^{-1}·s^{-1} for $k_{p,lower}^t$ at 20 °C. k_p^t determined in this work has an activation energy (28.9 kJ·mol^{-1}) between these two limiting values, with the absolute rate coefficient (k_p^t = 10.8 L·mol^{-1}·s^{-1} at 20 °C according to eq 10) also intermediate but much closer to the value for BA dimer polymerization.

Conclusion

The dependence of the apparent propagation rate coefficient, k_p^{app}, on pulse repetition rate has been measured for PLP of butyl acrylate at temperatures between −10 and 30 °C. At low repetition rates the k_p^{app} values are determined from the inflection point of the single peak in MWD. The backbiting rate coefficient, k_{bb}, at each temperature is determined from the sharp fall of k_p^{app} with decreasing laser pulse repetition rate. Via this novel approach, k_{bb} may be obtained without knowing any other rate coefficient. The dispersion parameter of SEC broadening, which is required for k_{bb} analysis, has been found by fitting measured MWDs, but may also be obtained from separate experiments. The k_{bb} estimates are fitted well by an Arrhenius relation resulting in a pre-exponential factor: $A(k_{bb}) = (4.84 \pm 0.29) \times 10^7$ s^{-1} and an activation energy: $E_a(k_{bb}) = (31.7 \pm 2.5)$ kJ·mol^{-1}, in close agreement with the literature values determined via ^{13}C NMR analysis of quaternary carbon atoms.

A procedure is also developed to estimate k_p^{av} from the values of k_p^{app} measured at low repetition rates, and thus calculate k_p^t, the rate coefficient for BA addition to the midchain radical. The resulting Arrhenius parameters, once again for the temperature range of −10 to 30 °C, are determined to be $A(k_p^t) = (1.52 \pm 0.14) \times 10^6$ L·mol^{-1}·s^{-1} and $E_a(k_p^t) = (28.9 \pm 3.2)$ kJ·mol^{-1}. These values indicate that propagation of acrylate dimer provides a good model for monomer addition to the midchain radical in this temperature range.

References and Notes

(1) Olaj, O. F.; Bitai, I.; Hinkelmann, F. *Macromol. Chem.* **1987**, *188*, 1689−1702.
(2) Schulz, G. V.; Romatowski, J. *Makromol. Chem.* **1965**, *85*, 195−226.
(3) (a) Aleksandrov, A. P.; Genkin, V. N.; Kitai, M. S.; Smirnova, I. M.; Sokolov, V. V. *J. Quantum Electron.* **1977**, *4*, 976−981. (b) Genkin, V. N.; Sokolov, V. V. *Dokl. Akad. Nauk SSSR* **1977**, *234*, 94−96.
(4) van Herk, A. M. *Macromol. Theory Simul.* **2000**, *9*, 433−441.
(5) Beuermann, S.; Buback, M. *Prog. Polym. Sci.* **2002**, *27*, 191−254.
(6) Buback, M.; Gilbert, R. G.; Hutchinson, R. A.; Klumperman, B.; Kuchta, F.-D.; Manders, B. G.; O'Driscoll, K. F.; Russell, G. T.; Schweer, J. *Macromol. Chem. Phys.* **1995**, *196*, 3267−3280.
(7) Beuermann, S.; Buback, M.; Davis, T. P.; Gilbert, R. G.; Hutchinson, R. A.; Olaj, O. F.; Russell, G. T.; Schweer, J.; van Herk, A. M. *Macromol. Chem. Phys.* **1997**, *198*, 1545−1560.
(8) Beuermann, S.; Buback, M.; Davis, T. P.; Gilbert, R. G.; Hutchinson, R. A.; Kajiwara, A.; Klumpermann, B.; Russell, G. T. *Macromol. Chem. Phys.* **2000**, *201*, 1355−1364.
(9) Beuermann, S.; Buback, M.; Davis, T. P.; Garcia, N.; Gilbert, R. G.; Hutchinson, R. A.; Kajiwara, A.; Kamachi, M.; Lacík, I.; Russell, G. T. *Macromol. Chem. Phys.* **2003**, *204*, 1338−1350.
(10) Asua, J. M.; Beuermann, S.; Buback, M.; Castignolles, P.; Charleux, B.; Gilbert, R. G.; Hutchinson, R. A.; Leiza, J. R.; Nikitin, A. N.; Vairon, J. P.; van Herk, A. M. *Macromol. Chem. Phys.* **2004**, *205*, 2151−2160.
(11) Davis, T. P.; O', Driscoll, K. F.; Piton, M. C.; Winnik, M. A. *Polym. Int.* **1991**, *24*, 65−70.
(12) Buback, M.; Degener, B. *Makromol. Chem.* **1993**, *194*, 2875−2883.
(13) Lyons, R. A.; Hutovic, J.; Piton, M. C.; Christie, D. J.; Clay, P. L.; Manders, B. G.; Kable, S. H.; Gilbert, R. G. *Macromolecules* **1996**, *29*, 1918−1927.
(14) Beuermann, S.; Paquet, D. A., Jr.; McMinn, J. H.; Hutchinson, R. A. *Macromolecules* **1996**, *29*, 4206−4215.
(15) Hutchinson, R. A.; Paquet, D. A., Jr.; McMinn, J. H.; Beuermann, S.; Fuller, R. E.; Jackson, C. *DECHEMA Monogr.* **1995**, *131*, 467−492.
(16) Manders, B. G. Ph.D. Thesis Dissertation, University of Eindhoven, Eindhoven, The Netherlands, 1997; Chapter 5, pp 51−88.
(17) Beuermann, S.; Buback, M.; Schmaltz, C. *Macromolecules* **1998**, *31*, 8069−8074.
(18) Beuermann, S.; Buback, M.; Schmaltz, C.; Kuchta, F.-D. *Macromol. Chem. Phys.* **1998**, *199*, 1209−1216.
(19) Buback, M.; Kurz, C. H.; Schmaltz, C. *Macromol. Chem. Phys.* **1998**, *199*, 1721−1727.

(20) Couvreur, L.; Piteau, G.; Castignolles, P.; Tonge, M.; Coutin, B.; Charleux, B.; Vairon, J. P. *Macromol. Symp.* **2001**, *174*, 197−207.
(21) Pierik, S. C. J.; van Herk, A. M.; Plessis, C.; van Steenis, J. H.; Loonen, T.; Bombeeck, A. *Eur. Polym. J.* **2005**, *41*, 1212−1218.
(22) de Kock, J. B. L. Ph.D. Thesis Dissertation, University of Eindhoven, Eindhoven, The Netherlands, 1999; Chapter 4, pp 121−186.
(23) Gilbert, B. C.; Lindsay Smith, J. R.; Milne, E. C.; Whitwood, A. C.; Taylor, P. *J. Chem. Soc., Perkin Trans.* **1994**, *2*, 1759−1769.
(24) Ahmad, N. M.; Heatley, F.; Lovell, P. A. *Macromolecules* **1998**, *31*, 2822−2827.
(25) Yamada, B.; Azukizawa, M.; Yamazoe, H.; Hill, D. J. T.; Pomery, P. J. *Polymer* **2000**, *41*, 5611−5618.
(26) Azukizawa, M.; Yamada, B.; Hill, D. J. T.; Pomery, P. J. *Macromol. Chem. Phys.* **2000**, *201*, 774−781.
(27) Plessis, C.; Arzamendi, G.; Leiza, J. R.; Schoonbrood, H. A. S.; Charmot, D.; Asua, J. M. *Macromolecules* **2000**, *33*, 4−7.
(28) Farcet, C.; Belleney, J.; Charleux, B.; Pirri, R. *Macromolecules* **2002**, *35*, 4912−4918.
(29) Plessis, C.; Arzamendi, G.; Alberdi, J. M.; van Herk, A. M.; Leiza, J. R.; Asua, J. M. *Macromol. Rapid Commun.* **2003**, *24*, 173−177.
(30) Willemse, R. X. E.; van Herk, A. M.; Panchenko, E.; Junkers, T.; Buback, M. *Macromolecules* **2005**, *38*, 5098−5103.
(31) Quan, C.; Soroush, M.; Grady, M. C.; Hansen, J. E.; Simonsick, W. J., Jr. *Macromolecules* **2005**, *38*, 7619−7628.
(32) Arzamendi, G.; Plessis, C.; Leiza, J. R.; Asua, J. M. *Macromol. Theory Simul.* **2003**, *12*, 315−324.
(33) Nikitin, A. N.; Castignolles, P.; Charleux, B.; Vairon, J.-P. *Macromol. Theory Simul.* **2003**, *12*, 440−448.
(34) Peck, A. N. F.; Hutchinson, R. A. *Macromolecules* **2004**, *37*, 5944−5951.
(35) Scott, G. E.; Senogles, E. *J. Macromol. Sci. Chem.* **1970**, *A4*, 1105−1117. Scott, G. E.; Senogles, E. *J. Macromol. Sci., Rev. Macromol. Chem.* **1973**, *C9* (1), 49−69. Scott, G. E.; Senogles, E. *J. Macromol. Sci. Chem.* **1974**, *A8*, 753−773.
(36) Wunderlich, W. *Makromol. Chem.* **1976**, *177*, 973−989.
(37) Kaszás, G.; Földes-Berezsnich, T.; Tüdös, F. *Eur. Polym. J.* **1983**, *19*, 469−473.
(38) Madruga, E. L.; Fernández-García, M. *Macromol. Chem. Phys.* **1996**, *197*, 3743−3755.
(39) McKenna, T. F.; Villanueva, A.; Santos, A. M. *J. Polym. Sci., Part A: Polym. Chem.* **1999**, *37*, 571−588.
(40) Fernández-García, M.; Fernández-Sanz, M.; Lopez Madruga, E. *Macromol. Chem. Phys.* **2000**, *201*, 1840−1845.
(41) Korolev, G. V.; Perepelitsina, E. O. *Polym. Sci., Ser. A* **2001**, *43*, 774−783.
(42) Nikitin, A. N.; Hutchinson, R. A. *Macromolecules* **2005**, *38*, 1581−1590.
(43) Nikitin, A. N.; Hutchinson, R. A. *Macromol. Theory Simul.* **2006**, *15*, 128−136.
(44) Nikitin, A. N.; Castignolles, P.; Charleux, B.; Vairon, J.-P. *Macromol. Rapid Commun.* **2003**, *24*, 778−782.
(45) Müller, M. Ph.D. Thesis, University of Göttingen, Göttingen, Germany, 2005.
(46) Castignolles, P. Ph.D. Thesis, University Pierre et Marie Curie, Paris, France, 2003.
(47) Buback, M.; Hesse, P.; Lacík, I. *Macromol. Rapid Commun.* **2007**, *28*, 2049−2054.
(48) Lacík, I.; Beuermann, S.; Buback, M. *Macromolecules* **2003**, *36*, 9355−9363.
(49) Lacík, I.; Beuermann, S.; Buback, M. *Macromol. Chem. Phys.* **2004**, *205*, 1080−1087.
(50) Sarnecki, J.; Schweer, J. *Macromolecules* **1995**, *28*, 4080−4088.
(51) Nikitin, A. N.; Castignolles, P.; Charleux, B.; Vairon, J.-P. Influence of intramolecular transfer to polymer on determination of propagation rate coefficients of alkyl acrylates by Pulsed Laser Polymerization. A lecture presented at the World Polymer Congress−Macro2004, Paris, France, July 4−9, 2004.
(52) Maeder, S.; Gilbert, R. G. *Macromolecules* **1998**, *31*, 4410−4418.
(53) Wulkow, M. *Macromol. Theory Simul.* **1996**, *5*, 393−416.
(54) Buback, M.; Busch, M.; Lämmel, R. A. *Macromol. Theory Simul.* **1996**, *5*, 845−861.
(55) Castignolles, P.; Nikitin, A. N.; Couvreur, L.; Mouraret, G.; Charleux, B.; Vairon, J.-P. *Macromol. Chem. Phys.* **2006**, *207*, 81−89.
(56) Moad, G.; Shipp, D. A.; Smith, T. A.; Solomon, D. H. *Macromolecules* **1997**, *30*, 7627−7630.
(57) Nikitin, A. N.; Hutchinson, R. A. *Macromol. Theory Simul.* **2007**, *16*, 29−42.
(58) Buback, M.; Müller, E. *Macromol. Chem. Phys.* **2007**, *208*, 581−593.
(59) Hakim, M.; Verhoeven, V.; McManus, N. T.; Dubé, M. A.; Penlidis, A. *J. Appl. Polym. Sci.* **2000**, *77*, 602−609.
(60) Li, D.; Grady, M. C.; Hutchinson, R. A. *Ind. Eng. Chem. Res.* **2005**, *44*, 2506−2517.

MA071413O